Cerebral Cortex, March 2018;28: 974–987

doi: 10.1093/cercor/bhx005
Advance Access Publication Date: 20 January 2017
Original Article

ORIGINAL ARTICLE

mGluR2 versus mGluR3 Metabotropic Glutamate Receptors in Primate Dorsolateral Prefrontal Cortex: Postsynaptic mGluR3 Strengthen Working Memory Networks

Lu E. Jin[1], Min Wang[1], Veronica C. Galvin[1], Taber C. Lightbourne[1], Peter Jeffrey Conn[2], Amy F.T. Arnsten[1] and Constantinos D. Paspalas[1]

[1]Department of Neuroscience, Yale University School of Medicine, New Haven, CT 06510, USA and [2]Department of Pharmacology and Vanderbilt Center for Neuroscience Drug Discovery, Vanderbilt University Medical Center, Nashville, TN 37232-0697, USA

Address correspondence to Constantinos D. Paspalas and Amy F.T. Arnsten, Department of Neuroscience, Yale University School of Medicine, 333 Cedar St, New Haven, CT 06510, USA. Email: constantinos.paspalas@yale.edu / amy.arnsten@yale.edu

Abstract

The newly evolved circuits in layer III of primate dorsolateral prefrontal cortex (dlPFC) generate the neural representations that subserve working memory. These circuits are weakened by increased cAMP-K^+ channel signaling, and are a focus of pathology in schizophrenia, aging, and Alzheimer's disease. Cognitive deficits in these disorders are increasingly associated with insults to mGluR3 metabotropic glutamate receptors, while reductions in mGluR2 appear protective. This has been perplexing, as mGluR3 has been considered glial receptors, and mGluR2 and mGluR3 have been thought to have similar functions, reducing glutamate transmission. We have discovered that, in addition to their astrocytic expression, mGluR3 is concentrated postsynaptically in spine synapses of layer III dlPFC, positioned to strengthen connectivity by inhibiting postsynaptic cAMP-K^+ channel actions. In contrast, mGluR2 is principally presynaptic as expected, with only a minor postsynaptic component. Functionally, increase in the endogenous mGluR3 agonist, N-acetylaspartylglutamate, markedly enhanced dlPFC Delay cell firing during a working memory task via inhibition of cAMP signaling, while the mGluR2 positive allosteric modulator, BINA, produced an inverted-U dose–response on dlPFC Delay cell firing and working memory performance. These data illuminate why insults to mGluR3 would erode cognitive abilities, and support mGluR3 as a novel therapeutic target for higher cognitive disorders.

Key words: Alzheimer's disease, dendritic spine, GRM2, GRM3, schizophrenia

Introduction

The newly evolved layer III pyramidal cell circuits in dorsolateral prefrontal cortex (dlPFC) subserve higher cognitive functions and are uniquely regulated at the molecular level, increasing vulnerability to dysfunction. Indeed, these dlPFC circuits are a target of pathology in schizophrenia, aging, and Alzheimer's disease (AD). These disorders have also been linked to insults in glutamate signaling. Data increasingly point to alterations in the group II metabotropic glutamate receptors, mGluR2 and mGluR3 (encoded by GRM2 and GRM3 genes, respectively), in association with dlPFC cognitive deficits in schizophrenia and aging. Until now, mGluR2 and mGluR3 have been thought to have very similar

functions: they share great sequence homology, generally couple to Gi/o signaling, and provide negative feedback to reduce glutamate signaling, whereby presynaptic mGluR2 inhibit glutamate release, while glial mGluR3 increase glutamate uptake by regulating excitatory amino acid transporters (EAATs) (Tanabe et al. 1992). Thus, it has been perplexing that cognitive disorders appear to be associated with reductions in mGluR3 but increases in mGluR2 function.

Insults that reduce mGluR3 expression and/or function are increasingly linked to impaired dlPFC cognitive abilities in schizophrenia (Harrison et al. 2008; Ghose et al. 2009), aging, and AD (Caraci et al. 2011). Genetic variations in GRM3 are associated with weaker dlPFC cognitive abilities and altered activation of dlPFC during performance of cognitive tasks (Egan et al. 2004). Postmortem brain studies from patients with schizophrenia have shown reduced mGluR3 expression, specifically in dlPFC, and increased expression of glutamate carboxypeptidase II, the extracellular enzyme that catabolizes the endogenous mGluR3 ligand N-acetylaspartylglutamate (NAAG) (Ghose et al. 2009). Taken together, these studies suggest that patients with schizophrenia may have much lower levels of mGluR3 stimulation in dlPFC. Importantly, the expression of GRM3 also decreases with advancing age in human dlPFC (Colantuoni et al. 2008), suggesting that it may contribute to age-related cognitive disorders. Animal models of AD have shown that mGluR3 is protective against beta-amyloid (Aβ) toxicity (Caraci et al. 2011), suggesting that reductions in mGluR3 with age may contribute to increased risk of AD. In contrast, mGluR2 promote Aβ toxicity in AD models (Caraci et al. 2011), and increase the risk of schizophrenia, as methylation of the GRM2 promoter that reduces mGluR2 expression is protective against the illness (Kordi-Tamandani et al. 2013). Given the apparent similarities between these receptors, why are mGluR3 beneficial and mGluR2 detrimental to our highest order cognitive functions? And, if mGluR3 is principally in astrocytes, why does their loss result in specific impairments of dlPFC cognitive abilities rather than a more generalized phenotype such as epilepsy? The key to these questions is likely in their exact placement within the dlPFC circuits that subserve higher cognitive processes, and in their differential influences on the functioning of these circuits.

Primate evolution has led to a great expansion in the number of glutamatergic synapses on pyramidal cells in deep layer III of dlPFC (Elston 2003), the circuits that generate mental representations underlying abstract thought (Goldman-Rakic 1995). These pyramidal cells, termed "Delay cells," recurrently excite each other through NMDAR synapses on long, thin dendritic spines to maintain neuronal firing in the absence of sensory stimulation, for example, during the delay epoch of working memory tasks. The tuning of visuospatial representation is refined through lateral inhibition by GABAergic interneurons (Fig. 1A–C). The majority of spines of layer III dlPFC pyramidal cells are mature, thin-type spines, a phenotype that may facilitate dynamic changes in connectivity (Arnsten et al. 2012). Indeed, a unique feature of these circuits is that their synaptic strength is rapidly weakened by cAMP-PKA opening of HCN and KCNQ K^+ channels on spines (Fig. 1D), for example, as occurs during uncontrollable stress (Arnsten et al. 2012). Immunoelectron microscopy (immunoEM) has identified a constellation of cAMP signaling proteins anchored next to the spine apparatus, that is, the extension and elaboration of the Ca^{2+}-storing smooth endoplasmic reticulum into the spine, positioned to mediate feedforward Ca^{2+}-cAMP signaling near the synapse (Paspalas et al. 2013). Conversely, inhibiting cAMP signaling strengthens connectivity and enhances Delay cell firing (Wang et al. 2007). These layer III pyramidal cell circuits are a focus of pathology in schizophrenia, where there is reduced number of dendritic spines (Glantz and Lewis 2000). The same neurons are also vulnerable to age-related spine loss (Morrison and Baxter 2012) and age-related reduction in neuronal firing from disinhibited cAMP-K^+ channel signaling (Wang et al. 2011). The dlPFC is also a focus of AD pathology, where layer III pyramidal cells undergo neurofibrillary degeneration (Morrison and Baxter 2012). Thus, pinpointing glutamate actions within these dlPFC circuits is of great clinical significance.

This study dissected mGluR2 versus mGluR3 localization and actions in the primate dlPFC layer III circuits that underlie higher cognition, and examined their influence on Delay cell firing and working memory function. Results revealed an unexpected concentration of mGluR3 in dendritic spines, and a remarkable enhancement of neuronal firing with mGluR3 stimulation, explaining why genetic or environmental insults to mGluR3 would impair cognitive function.

Materials and Methods

All procedures were in accordance with NIH guidelines and approved by the Yale University IACUC.

Immunoelectron Microscopy

Four female adult Rhesus macaques (9–11 years) were perfused transcardially with artificial cerebrospinal fluid, followed by 4% paraformaldehyde, 0.05% glutaraldehyde, and 0.18% picric acid in 0.1 M phosphate buffer. The brains were vibrosliced coronally at 70 μm, and sections of dlPFC were processed with peroxidase or/and silver-enhanced 1.4 nm gold for single and dual immunocytochemistry. All immunoprocedures as well as processing for electron microscopy have been described previously (Wang et al. 2007; Paspalas et al. 2013).

The mGluR2-specific antibody was raised in rabbits against amino acids 109–121 of rat mGluR2 N-terminus with 100% sequence homology with monkey mGluR2 (0.16 μg/mL; AGC-011, Alomone). The mGluR3-specific rabbit antibody was raised against a sequence within the N-terminus of human mGluR3 (12.5 μg/mL; G1545, Sigma-Aldrich). An array of nonrabbit antibodies (including avian IgY) were also tested but performed poorly, and, therefore, for dual immunocytochemistry, we relied on antibodies from the same species but modified with monovalent Fab as detailed below.

Dual immunolabeling against mGluR2 and mGluR3 was performed combining peroxidase and silver-enhanced ultrasmall gold. Primary antibodies were produced in rabbit, which necessitated a modification of the immunoprocedure, plus an additional series of controls due to species cross-reactivity. More specifically, sections were incubated in the first primary antibody, followed by a goat anti-rabbit secondary antibody conjugated to 1.4 nm gold (1:200; Nanoprobes). Subsequently, the sections were incubated with an excess of goat anti-rabbit Fab monovalent fragments (1:50; Jackson Immunoresearch), to block remaining antigenicity of the first primary antibody, and postfixed for 10 min in 2% paraformaldehyde. Sections were then transferred to the second primary antibody, followed by goat anti-rabbit biotinylated secondary antibody (1:500; Jackson Immunoresearch). The immunocomplexes were fixed for 10 min with 1% glutaraldehyde in PB and the gold was silver enhanced (HQ Silver, Nanoprobes), to visualize the first primary antibody. The avidin-biotinylated peroxidase complex (1:200; Vector Laboratories) was used next to visualize the second primary antibody with 0.05% diaminobenzidine as a chromogen.

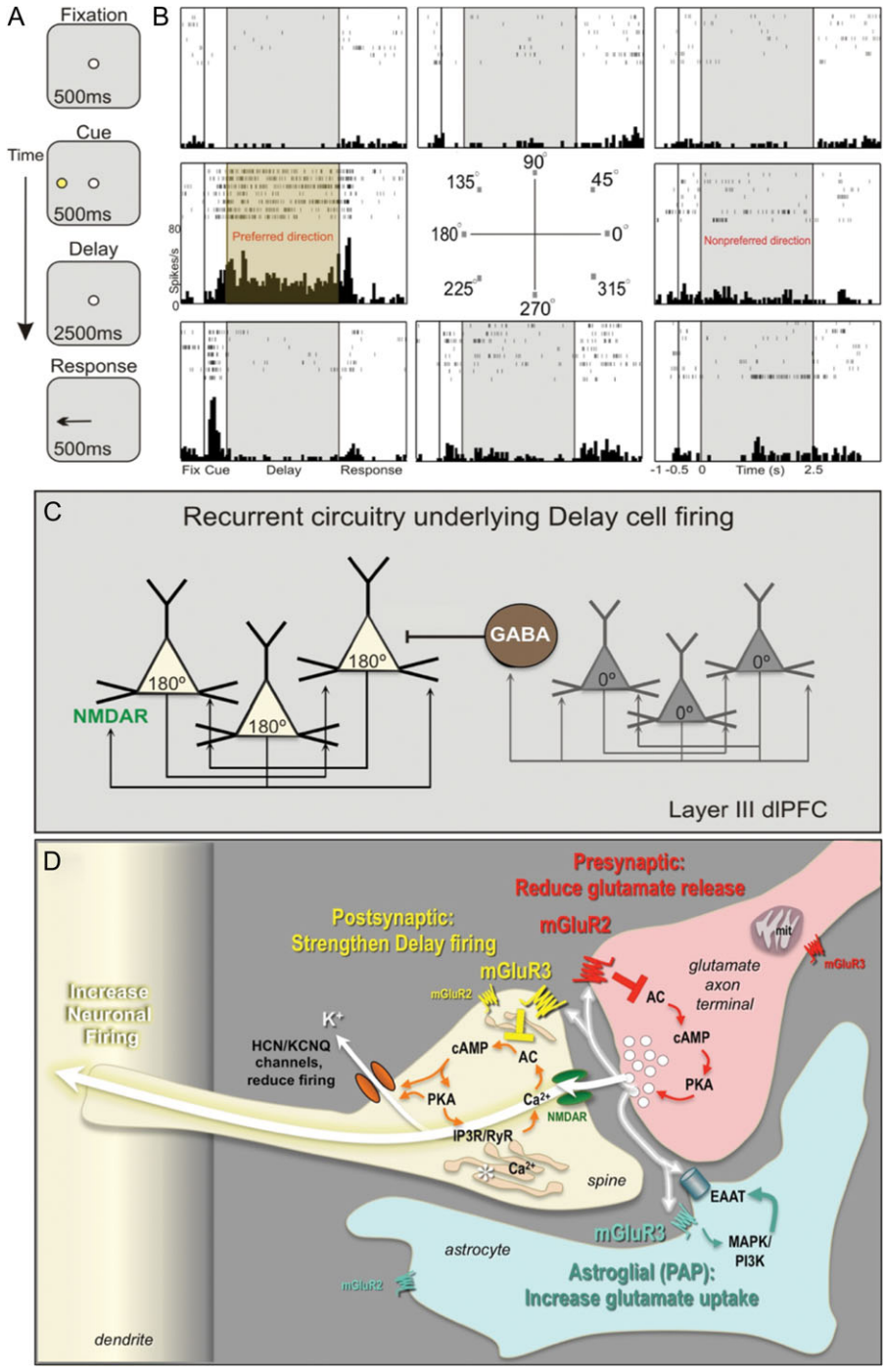

Figure 1. Neuronal basis of visuospatial representation during a working memory task. (*A*) The ODR task. The monkey initiates a trial by fixating a central point; a visual cue appears at 1 of 8 locations; the monkey must remember the cued location over a delay period and make a saccade to the correct location to get reward. The cued location varies from trial to trial, requiring constant updating of information held in working memory. (*B*) A typical Delay cell, with spatially tuned persistent firing across the delay period in the neuron's preferred direction (180°) but not for nonpreferred directions (e.g., 0°). (*C*) Deep layer III dlPFC microcircuits that generate Delay cell firing. Pyramidal neurons with similar preferred directions excite each other through NMDAR synapses, for example, a cluster of 180° neurons maintain firing across the delay following a cue at 180°, but reduce firing at 0° (nonpreferred direction) via lateral inhibition from GABAergic interneurons. (*D*) Working model of mGluR2 and mGluR3 actions in a layer III dlPFC glutamatergic synapse. Postsynaptic mGluR3 reside near the synapse and mGluR2 near the Ca^{2+}-storing spine apparatus (asterisk). They inhibit cAMP production, close HCN and KCNQ channels, strengthen synaptic efficacy, and enhance Delay cell firing. In contrast, presynaptic mGluR2 on axon terminals reduce glutamate release. mGluR3 on PAPs increase glial glutamate uptake by increasing EAAT expression via mitogen-activated protein kinase and phosphoinositide 3-kinase signaling (Aronica et al. 2003). The functions of presynaptic mGluR3 near mitochondria, and of mGluR2 on astrocytes at a distance from the synapse are unknown.

The peroxidase and gold dual immunoprocedure (without the monovalent Fab modification) has been described in detail previously (Wang et al. 2007; Paspalas et al. 2013).

Effective blocking of species cross-reactivity was evaluated for all antigen pairs under the electron microscope. To exclude bias, antigens within pairs were also reversed so that an antigen that was gold-labeled in one series was labeled with peroxidase in a parallel series of experiments. The pattern of localization of either receptor in dual labeling was identical to the corresponding pattern revealed with single immunolabeling (see Fig. 2). Omission of the first primary antibody or substitution with nonimmune rabbit serum eliminated the gold signal, and, similarly, omission/substitution of the second primary antibody eliminated peroxidase labeling. For comparison, omission/substitution control experiments where the monovalent Fab modification was not used resulted in signal overlap due to both secondary antibodies binding to a single primary antibody.

Quantitative assessments were performed on peroxidase-labeled material using random, 21.6 μm^2 fields of the dlPFC neuropil (original magnification ×30 000), captured from the fourth surface-most ultrathin section of each plastic block; 5 fields/block, 5 blocks/brain for the total of 4 brains. An area of 2160 μm^2 was sampled for each receptor, where 605 mGluR2 and 699 mGluR3 cellular profiles were identified. A detailed account of serial section analysis and the criteria for categorizing the dendritic spines are described in Paspalas et al. (2013).

Electrophysiology and Iontophoresis

Oculomotor Delayed Response Task

Two male adult Rhesus macaques (12 and 17 years) were trained to perform an oculomotor delayed response (ODR) task, a test of visuospatial working memory. In ODR, the monkey must remember the location of a briefly presented cue over a delay period, and then make an eye movement to the correct location to receive liquid reward (Fig. 1A). The cued location varies from trial to trial, requiring constant updating of the spatial information held in working memory.

In detail, a central spot is illuminated on an LED monitor, serving as the fixation target. The animal begins a trial by maintaining fixation at the central spot for 0.5 s (fixation period). Then, a cue is illuminated for 0.5 s (cue period) at 1 of 8 peripheral targets located at an eccentricity of 13° with respect to the fixation spot, followed by a 2.5 s delay period. During the cue and delay period, the animal is required to maintain fixation at the central spot. The fixation spot is extinguished at the end of the delay period, instructing the monkey to make a memory-guided saccade to the remembered location. A trial was considered successful if the animal made a saccade to the area within 2° around the previously cued location, and within 0.5 s after the offset of the fixation spot, which was rewarded with juice immediately after a successful response. The inter-trial interval was 3 s. The animal's eye position was monitored with the ISCAN Eye Movement Monitoring System (ISCAN), and the ODR task was generated by PictoBox System (developed by Dr Daeyeol Lee and colleagues, Yale University).

Recording Site

Animals underwent a magnetic resonance imaging (MRI) brain scan in order to obtain the exact anatomical coordinates, which were then used to guide placement of the chronic recording chambers. MRI-compatible materials were used for the implant so that future MRI scans could be performed after implantation to confirm the position of the recording chambers over the caudal principal sulcus of cortical area 46.

Pharmacology

The following drugs were used in this study: (1) the mGluR2-selective positive allosteric modulator (PAM), biphenylindanone A (BINA) potassium salt, (2) the mGluR3-selective agonist, NAAG (also called spaglumic acid), and (3) the glutamate carboxypeptidase II and III inhibitor, ZJ43. BINA was custom made in salt formulation by Tocris Bioscience for these experiments. NAAG was purchased from Sigma-Aldrich and ZJ43 was from Tocris. Drugs were dissolved in distilled water (pH adjusted to 7.5–8.5 for NAAG and ZJ43).

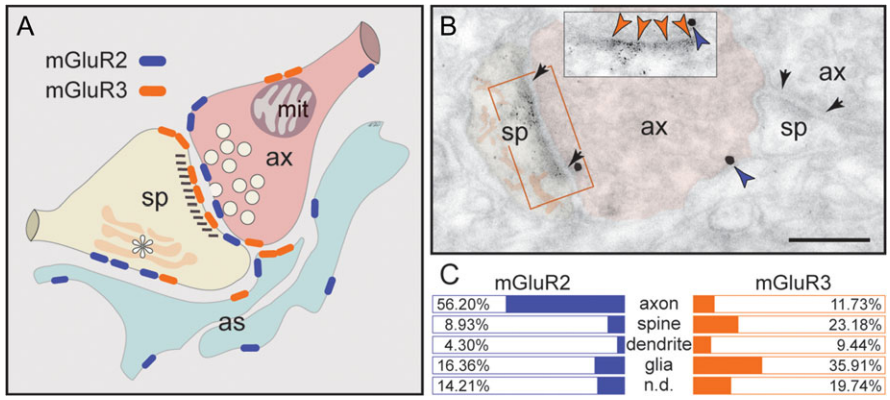

Figure 2. Summary of mGluR2 versus mGluR3 expression patterns in layer III dlPFC. (*A*) mGluR2 is principally a presynaptic receptor, targeted to synapses as well as preterminal axons. Postsynaptic expression is limited to extrasynaptic spine membranes, in association with the spine apparatus (asterisk), and rarely to perisynaptic membranes. Neuronal mGluR3 is primarily a postsynaptic receptor targeted to long, thin spine synapses, the spine type that is (1) most prevalent in layer III dlPFC, (2) most associated with cAMP-K^+ channel modulation, and (3) most vulnerable to loss with advancing age. In contrast, there is little presynaptic expression of mGluR3, specifically along the axonal membrane facing mitochondria (mit) and rarely perisynaptically. Both mGluR2 and mGluR3 are localized in astrocytes in primate dlPFC. The localization of mGluR2 in glia is distinct from mGluR3, as it is not targeted to the glial leaflets ensheathing the synapse, which is the typical mGluR3 pattern. (*B*) Dual immunolabeling for mGluR2 (immunogold, blue arrowheads) and mGluR3 (DAB, orange arrowheads) reveals presynaptic mGluR2 and postsynaptic mGluR3 juxtapositioned at the same axospinous synapse (frame and inset). The labeled axon (ax) and spine (sp) are pseudocolored for clarity. A nonlabeled axospinous synapse is shown for comparison; synapses are between arrows. Scale bar, 200 nm. (*C*) The prevalence of mGluR2 versus mGluR3 in various cellular profiles in layer III of the dlPFC neuropil, expressed as percentage of an mGluR2 or mGluR3 profile (e.g., axon) per total mGluR2 or mGluR3 profiles, respectively (see quantitative assessment in the "Materials and Methods" section). Nondetermined (n.d.) are profiles that could not be unequivocally categorized.

Recording and Iontophoresis

Iontophoretic electrodes were constructed with a 20 μm-pitch carbon fiber (ELSI) inserted in the central barrel of a 7-barrel nonfilamented capillary glass (Friedrich and Dimmock). The assembly was pulled using a custom electrode puller (PMP-107, Microdata Instrument Inc.) and the tip was beveled to reach impedances of 0.3–1.0 MΩ with tip sizes of 30–40 μm. The outer 6 barrels of the electrode were then filled with up to 3 different drug solutions (2 consecutive barrels for each drug), which were pushed through the tip of the electrode using air. A Neurophore BH2 iontophoretic system (Medical Systems Corp.) was used to deliver the drugs. The drugs were ejected at currents that varied from 5 to 100 nA. Retaining currents of 5 nA at the opposite polarity were used in a cycled manner (1 s ON, 1 s OFF) when not applying drugs. Drug ejection did not create noise in the recording, and there was no iontophoresis-related change in spike waveforms at any ejection current. Iontophoretic application did not cause any observable behavioral changes either.

The electrode was mounted on a MO-95 micromanipulator (Narishige) in a 25-gauge stainless steel guide tube. The dura was punctured using the guide tube to enable the access of the electrode to the cortex. Extracellular voltage was amplified using a custom low-noise preamplifier (SKYLAB) and band-pass filtered (180 Hz–6 kHz, 20 dB gain, 4-pole Butterworth; Kron-Hite). Signals were digitized (15 kHz; micro 1401, CED) and acquired using the Spike2 software (CED). Neural activity was analyzed using Spike2 with waveform sorting by a template-matching algorithm, which made it possible to isolate multiple single units at the same recording site. Post-stimulus time histograms and rastergrams were constructed online to determine the relationship of unit activity to the task. Unit activity was measured in spikes per second. If the rastergrams displayed task-related activity, the units were recorded further and pharmacological testing was performed. Delay cells were identified as those with spatially tuned, persistent firing across the delay epoch (see, e.g., in Fig. 1*B*).

Following stable recording of a Delay cell under control conditions, pharmacological agents were applied via iontophoresis. Dose-dependent effects of the drugs were tested in 2 or more consecutive conditions. Drugs were continuously applied at a relevant current throughout a given condition, with ~8 trials per condition at each location for statistical analyses of drug effects. After the completion of recording, neural activity was analyzed again using a stricter waveform sorting and template-matching algorithm, which separated single units for future analysis. Data were analyzed using MATLAB (The MathWorks) and SPSS Statistics v23 (IBM). d' was calculated as a measure of the strength of spatial tuning using the formula: $d' = (\text{mean}_{\text{pref}} - \text{mean}_{\text{nonpref}})/\sqrt{(\text{sd}^2_{\text{pref}} + \text{sd}^2_{\text{nonpref}})/2}$. To test drug effects, we used repeated 1-way or 2-way ANOVA and 2-tailed paired-samples *t*-test. $P < 0.05$ was predetermined as the threshold for statistical significance.

Behavioral Assessments

The effects of systemically administered BINA were examined in young adult (9–17 years) and aged (18–30 years) female and male Rhesus macaques. Monkeys were trained on a manual, multiple delay spatial working memory task in a Wisconsin General Testing Apparatus. The animal watched the experimenter place food reward in 1 of 2 wells. The food wells were then covered with identical cardboards and an opaque screen was lowered for a delay period. The screen was then raised and the animal must point to the correct well to get reward. Reward was quasi-randomly distributed between the left and right wells, and a daily test session included 30 trials. Five different delay lengths (designated *A*, *B*, *C*, *D*, and *E* delays) were quasi-randomly distributed during a single test session, for example, $A = 0$, $B = 10$, $C = 20$, $D = 30$, and $E = 40$ s or $A = 0$, $B = 5$, $C = 10$, $D = 15$, $E = 20$ s. All monkeys performed near perfectly at 0 s, where the opaque screen was not lowered, and exhibited increasing errors with longer delays. The delay lengths were adjusted for each animal so that they had a stable baseline performance of 67–80% correct. Occasionally, 3 or more wells were used for a few monkeys to keep their performance at baseline, without lengthening the delay. An animal received drug treatments if it had baseline performance for 2 consecutive test sessions.

Monkeys received vehicle or BINA doses 0.0001–0.05 mg/kg 60 min before testing. Higher doses (0.1–1.0 mg/kg) were piloted in a subset of monkeys to ensure that an effective dose range was not missed. Two of the 12 monkeys reliably ate drug/vehicle following oral administration; the remaining 10 monkeys primarily received intramuscular injections. A custom synthesized salt formulation of BINA was used for most treatments, and was dissolved and diluted in saline for intramuscular injections and in water for oral administration. A subset of treatments utilized standard BINA dissolved in DMSO and diluted in water. The highest doses (0.1–1.0 mg/kg) of the standard formulation could not be dissolved in water and thus were administered orally. No differences were seen between drug formulations and thus both are included in the current analysis. Monkeys were tested by experimenters blind to drug versus vehicle conditions, with washout periods of at least 10 days between drug treatments. Data were analyzed using SPSS statistics. Drug effect was tested with repeated 1-way ANOVA and 2-tailed paired-samples *t*-test. $P < 0.05$ was predetermined as the threshold for statistical significance.

Results

This study utilized a three-prong approach: (1) single and dual immunoEM, to localize mGluR2 versus mGluR3 in monkey layer III dlPFC circuits; (2) iontophoresis coupled with single-unit recordings in monkeys performing a spatial working memory task, to determine how agents that stimulate mGluR2 versus mGluR3 influence Delay cell firing; and (3) systemic administration of an mGluR2-selective PAM in monkeys, to observe its influence on spatial working memory performance.

Differential Subcellular Localization of mGluR2 versus mGluR3 in dlPFC

The ultrastructural location of mGluR2 and mGluR3 in layer III neuropil of the rhesus monkey dlPFC was determined using immunoperoxidase and/or 1.4 nm gold after silver enhancement. Figure 2 summarizes the subcellular distribution (Fig. 2*A*,*B*) and the prevalence (Fig. 2*C*) of mGluR2 versus mGluR3 at the plasma membrane of axons, dendritic spines, dendritic shafts and astrocytic processes.

mGluR3 is the Predominant Postsynaptic Receptor in Spines

Although previous studies of neuronal group II mGluR have focused on presynaptic receptors, the predominant localization of neuronal mGluR3 in dlPFC is in dendritic spines (Fig. 2*C*). The receptor is postsynaptic to glutamatergic-like synapses, where it is found within the synapse per se as well as perisynaptically (Fig. 3), and is often captured next to the spine apparatus (Fig. 3*F*,*G*).

Note that mGluR3 exhibits nonuniform expression along the length of the synaptic active zone or at the split active zones of a perforated synapse (Fig. 3*D–F*). Serial sections to visualize the spine neck revealed that postsynaptic mGluR3 concentrate in mature, thin-type dendritic spines containing a spine apparatus; stubby or mushroom-type spines were not labeled. Figure 3*G* typifies the mGluR3-reactive dendritic spine, where mGluR3 associates with the synapse as well as with the spine apparatus extending into the spine neck. Dendritic shafts expressed only weak mGluR3 immunoreactivity within glutamatergic-like synapses and at nonsynaptic membranes (Supplementary Fig. 1).

A limited postsynaptic component of mGluR2 is also captured in dendritic spines (Fig. 2*C*). Contrary to mGluR3 localization in thin-type spines, mGluR2 is found in a variety of spine types. The receptor is typically extrasynaptic, that is, not localized at the synaptic membrane, and only rarely appears perisynaptically in stubby and mushroom-type dendritic spines (Fig. 4*A,B*). Instead, mGluR2 is captured along sections of the plasma membrane in juxtaposition with the spine apparatus endomembranes. A strict, one-to-one association of extrasynaptic mGluR2 with the spine apparatus is visualized in Figure 4*C,D*.

mGluR2 is the Predominant Presynaptic Receptor

In contrast to its modest expression in dendritic spines, mGluR2 is prominently localized in glutamatergic-like axon terminals (Fig. 2*C*), where it presumably functions as an autoreceptor. mGluR2 is targeted to the synaptic active zone (Fig. 5*A*) or localized perisynaptically bordering the excitatory synapse (Fig. 5*A–D*). In addition to its major synaptic component, mGluR2 in axons appears extrasynaptically at sites remote from the synapse (Fig. 5*A–C*, Supplementary Fig. 2*A,B*). Bundled preterminal axons commonly expressed mGluR2 (Supplementary Fig. 2*C,D*), and such intervaricose segments were captured in continuity with glutamatergic-like axon terminals establishing axospinous synapses (Supplementary Fig. 2*A*).

Unlike the predominantly presynaptic mGluR2, axons represent only a small fraction of mGluR3-immunoreactive profiles in dlPFC (Fig. 2*C*). Presynaptic mGluR3 is typically extrasynaptic and found on small patches of the axonal plasma membrane (Fig. 5*E–G*), which, intriguingly, associate with apposing mitochondria (Fig. 5*E,F*). The receptor is seldom perisynaptic in axospinous synapses; one rare synaptic triad where mGluR3 flanks the glutamatergic-like synapse is shown in Figure 5*H*.

mGluR3 is the Predominant Glial Receptor in Astrocytic Processes

As expected from previous research, the predominant location of mGluR3 in layer III dlPFC is in astrocytes (Fig. 2*C*), targeted to the perisynaptic astrocytic processes (PAPs) ensheathing axospinous and, occasionally, axodendritic glutamatergic-like synapses. In fact, mGluR3 is not uniformly distributed along the PAP membranes but is concentrated next to the synapse (Fig. 6*A,B*), placing the receptor in the path of escaping glutamate. Consistent with its distribution in the neuropil, mGluR3 is found in the soma of astrocytes, in association with the synthetic machinery, that is, the rough endoplasmic reticulum and the Golgi complex (Supplementary Fig. 3*A*).

Unexpectedly, astrocytic plasma membranes were labeled against mGluR2 (Fig. 6*C,D*), although this expression was weak and not easily discerned. In support of a glial mGluR2 component, astrocytic somata were also weakly reactive

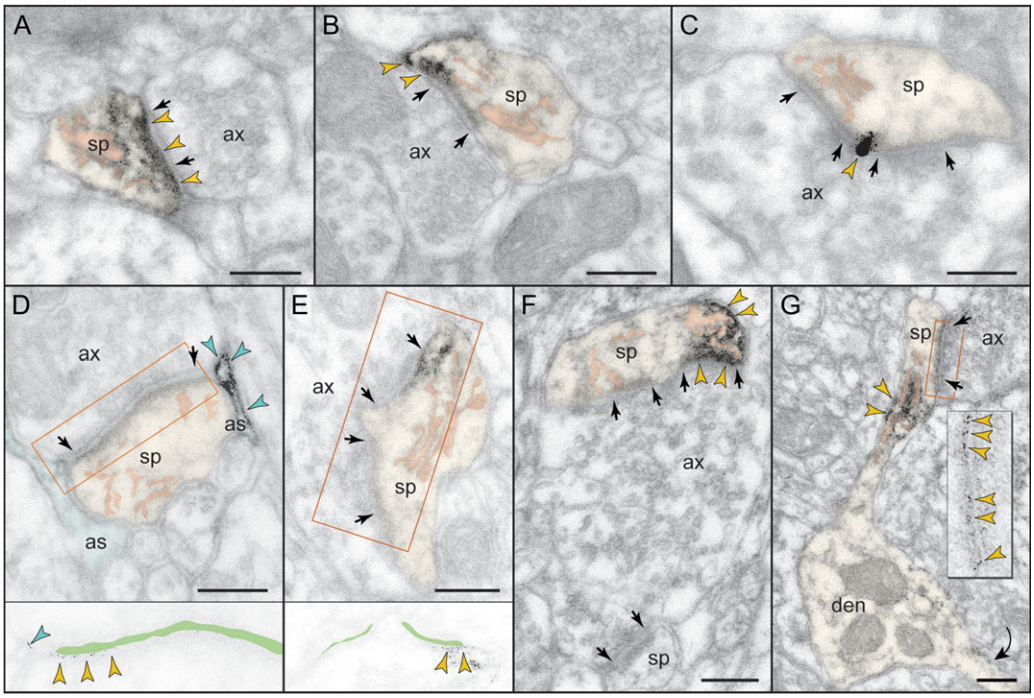

Figure 3. Postsynaptic expression of mGluR3 in monkey dlPFC. mGluR3 is prominently expressed in dendritic spines, both within the synaptic active zone (*A*) and perisynaptically (*B,C*); label in *C* is found at the central perforation of a perforated synapse. (*D,E*) The framed images are edited to facilitate receptor visualization at the synapse (the synaptic cleft is marked in green). Note in *D* the typical mGluR3 localization in PAPs. (*F,G*) mGluR3 is additionally expressed at nonsynaptic spine membranes. In *F*, one section of a perforated synapse is additionally labeled. Extrasynaptic mGluR3 in *G* is found next to the spine apparatus (pink-pseudocolored) in the spine neck of a prototypical thin spine; a second spine, not shown in its entirety, emanates from the parent dendrite (curved arrow). The enlarged frame in *G* shows the common postsynaptic expression of mGluR3 at the synapse. Labeled spines (sp) and astrocytes (as) are pseudocolored for clarity; color-coded arrowheads point to mGluR3; synapses are between arrows. ax, axon; den, dendrite. Scale bars, 200 nm.

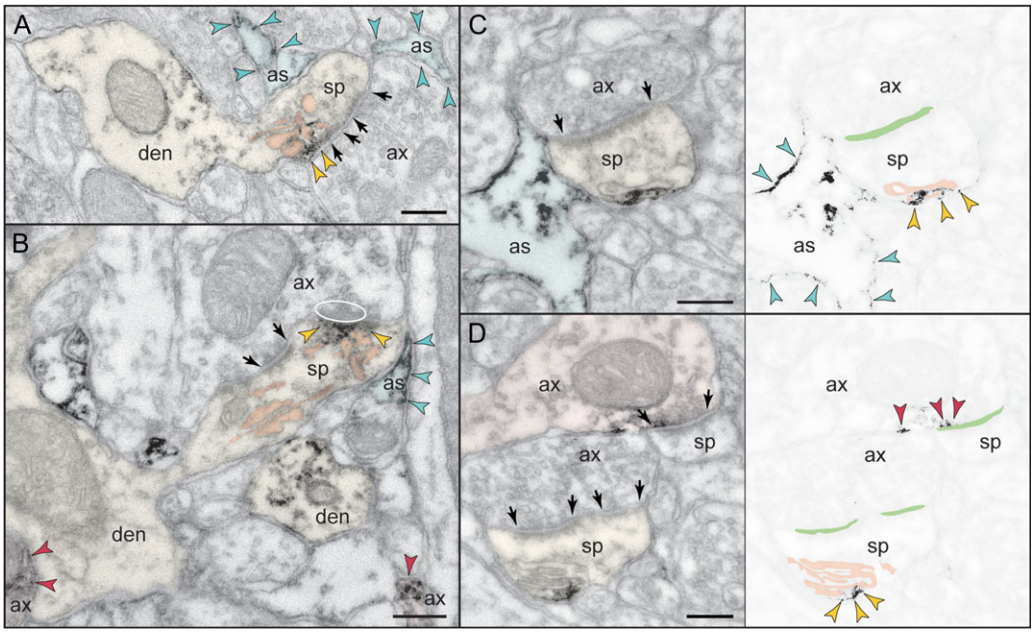

Figure 4. Postsynaptic expression of mGluR2 in monkey dlPFC. (*A*,*B*) mGluR2 is weakly expressed in dendritic spines perisynaptically. Its association with the glutamatergic-like synapse is selective to stubby (*A*) and mushroom-type (*B*) spines; in *B*, the obliquely sectioned synaptic disk is marked with oval. (*C*,*D*). However, mGluR2 in spines is primarily an extrasynaptic receptor. Remarkably, mGluR2 was distinctly associated with the plasma membrane facing the spine apparatus. This is best appreciated in the edited images *C* and *D*, where the synaptic cleft is marked in green and the apparatus is pink-pseudocolored. Note also the astrocytic as well as axonal labeling for mGluR2. Labeled axons (ax), dendrites (den), spines (sp), and astrocytes (as) are pseudocolored for clarity; color-coded arrowheads point to mGluR2; synapses are between arrows. Scale bars, 200 nm.

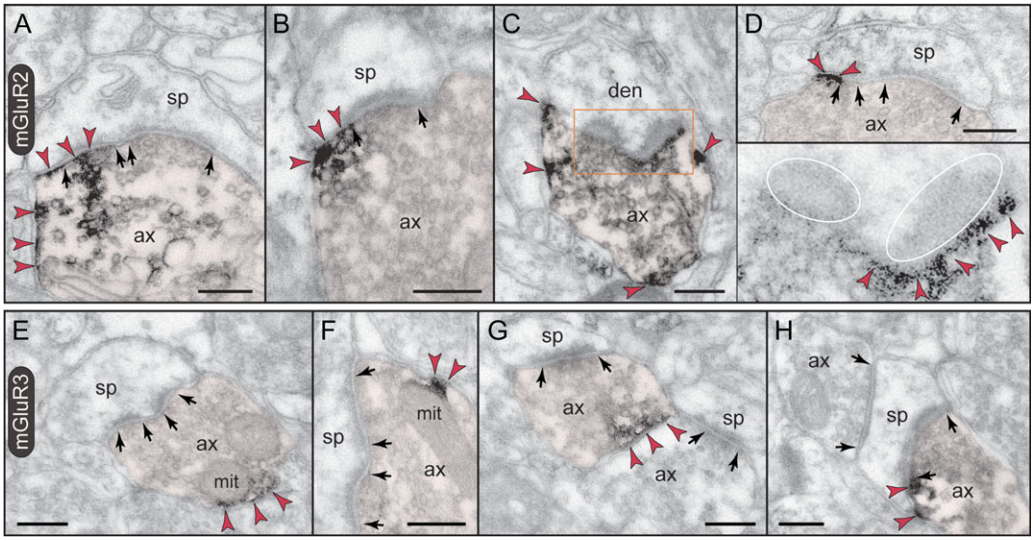

Figure 5. Presynaptic expression of mGluR2 versus mGluR3 in monkey dlPFC. (*A*–*D*) mGluR2 is expressed in glutamatergic-like axons establishing asymmetric synapses. Label is found within the synaptic active zone, and is typically over one section of a perforated synapse (*A*). Perisynaptic mGluR2 is visualized on membranes flanking the synapse (cross section in *B* and *D*) or in a halo surrounding the synaptic disk (ovals; oblique section in *C* and inset). Note that mGluR2 is also present extrasynaptically (*A*–*C*), and in preterminal axons (not captured here; see Supplementary Fig. 2). (*E*–*H*) Axons are weakly reactive against mGluR3. Unlike mGluR2, label is restricted to patches of the plasma membrane with a predilection for membranes apposing mitochondria (mit in *E* and *F*). As seen in *E*–*G*, axonal mGluR3 is for the most part extrasynaptic. However, there are rare examples when mGluR3 can be found perisynapticaly as in the synaptic triad in *H*. Labeled axons (ax) are pseudocolored for clarity; color-coded arrowheads point to mGluR2 or mGluR3; synapses are between arrows. den, dendrite; sp, spine. Scale bars, 200 nm.

(Supplementary Fig. 3B). However, unlike mGluR3, mGluR2 was not specifically targeted to PAPs but rather was distributed in astrocytic processes throughout the neuropil (Fig. 6C). When present in PAPs, mGluR2 was not concentrated at the synapse interface (Fig. 6D, compare with mGluR3 in Fig. 6B). This pattern of expression was confirmed in serial sections, where mGluR2 on astrocytic processes was not selectively associated with synapses in successive section planes.

Summary of ImmunoEM Findings

As summarized in Figure 2, mGluR3 is concentrated postsynaptically in thin-type spines, with limited presynaptic localization

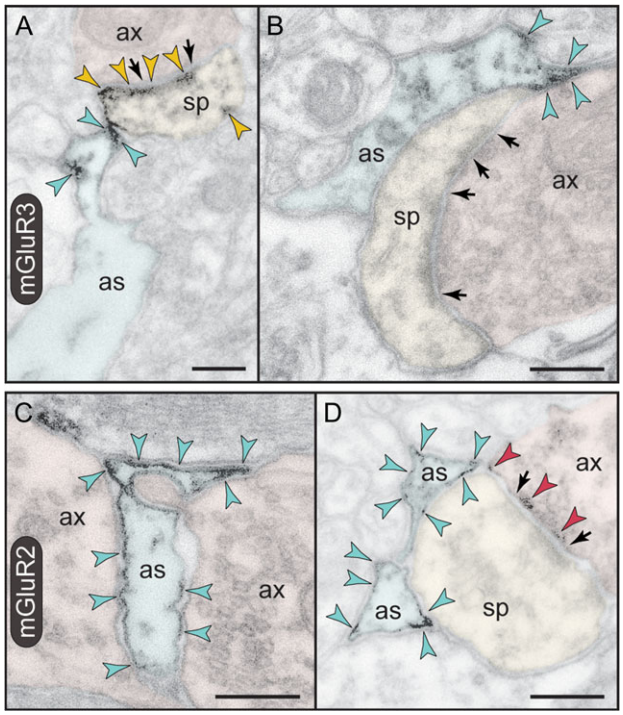

Figure 6. Astrocytic expression of mGluR3 versus mGluR2 in monkey dlPFC. (*A*,*B*) PAPs are selectively labeled for mGluR3; note that the receptor is not distributed uniformly on the PAP plasma membrane but is placed immediately next to the synapse in the path of escaping glutamate. A spine in *A* is also reactive against mGluR3 at the synapse, perisynaptically, and extrasynaptically. (*C*,*D*) In contrast to mGluR3, mGluR2 is not targeted to the PAPs ensheathing the synapse, but presents a more uniform distribution on astrocytic membranes. In *D*, presynaptic mGluR2 is also captured at the synapse. Axons (ax), spines (sp), and astrocytes (as) are pseudocolored for clarity; color-coded arrowheads point to mGluR3 or mGluR2; synapses are between arrows. Scale bars, 200 nm.

near mitochondria. In contrast, mGluR2 is predominantly presynaptic in glutamatergic-like axons, with limited postsynaptic expression in a variety of spine types. The combination of presynaptic mGluR2 and postsynaptic mGluR3 in a single axospinous synapse is captured in Figure 2*B* using dual immunolabeling. Astrocytes not only present the predicted mGluR3 in PAPs, but also express an unexpected mGluR2 component, which is not directly linked to synaptic glutamate and whose function is unknown. Importantly, the localization of mGluR3, and occasional mGluR2, on dendritic spine membranes near the spine apparatus suggests a key placement to strengthen connectivity of Delay cell recurrent excitatory networks.

Differential Actions of mGluR3 versus mGluR2 on dlPFC Delay Cell Firing

The effects of mGluR3 versus mGluR2 selective compounds on Delay cell firing were examined in monkeys performing the ODR test of visuospatial working memory. Although there are many mixed mGluR2/3 agonists, the great sequence homology between mGluR2 and mGluR3 has been a challenge to the development of compounds that dissect mGluR2 versus mGluR3 actions. As there are currently no selective PAMs for mGluR3, we used the endogenous ligand for mGluR3, NAAG, which is co-released with glutamate at axon terminals (Neale et al. 2011). Results with exogenous application of NAAG were compared with increasing endogenous levels of NAAG by inhibiting its catabolic enzyme, glutamate carboxypeptidase II, with ZJ43. The role of cAMP signaling was tested by challenging with the cAMP analog, 8-Bromo-cAMP. Finally, the effects of NAAG were compared with the first mGluR2-selective PAM, BINA, originally created by the Vanderbilt Center for Neuroscience Drug Discovery (Benneyworth et al. 2007).

mGluR3 Stimulation Enhances Delay Cell Firing

Iontophoresis of the endogenous mGluR3 ligand, NAAG, produced a robust and linear increase in Delay cell firing. An example is illustrated in Figure 7A, where NAAG (5–100 nA) produced a linear enhancement of neuronal firing. The neuron reduced its firing under the washout condition when NAAG was no longer applied (recovery).

Dose-related increases in firing can be seen following iontophoresis of NAAG for the averaged population of Delay cells (n = 22, Fig. 7*B*). The averaged firing rate showed a linear increase in delay-related firing with increasing dose compared with control conditions (1-ANOVA-R Huynh-Feldt corrected for sphericity, $F(1.2,25.7) = 5.603$, $P = 0.02$); linear trend, $F(1,21) = 7.423$, $P = 0.013$), with significant increases following both low (5–30 nA) and higher (50–100 nA) doses of NAAG (n = 22, low dose: $t_{dep}(21) = -4.362$, $P < 0.001$; high dose: $t_{dep}(21) = -2.725$, $P = 0.013$; low vs. high dose $P > 0.2$). The increases in delay-related firing were particularly prominent for the neurons' preferred direction, leading to an improvement in spatial tuning compared with control conditions as evidenced by significant spatial direction × drug interactions for both low doses (2-ANOVA-R, $F_{direction \times drug}(1,21) = 14.782$, $P = 0.001$) and high doses (2-ANOVA-R, $F_{direction \times drug}(1,21) = 14.782$, $P = 0.001$). Enhanced spatial tuning was also evident in measures of d' (Fig. 7*C*). Overall, NAAG doses produced a linear increase in d' (1-ANOVA-R, $F(2,42) = 3.718$, $P = 0.033$; linear trend, $F(1,21) = 4.628$, $P = 0.043$). Measures of d' were increased by either low doses ($t_{dep}(21) = -3.03$, $P = 0.006$) or high doses ($t_{dep}(21) = -2.151$, $P = 0.043$); d' measures following low versus high doses did not differ from each other ($P > 0.7$). As NAAG is a naturally occurring substance that can be hydrolyzed, the "high" doses may have been reduced to more physiologically appropriate levels by local neurons. In summary, both low and high doses of the mGluR3 agonist, NAAG, markedly enhanced Delay cell firing and spatial tuning, improving the representation of visual space by working memory circuits.

Increasing endogenous levels of NAAG through iontophoresis of the glutamate carboxypeptidase II inhibitor, ZJ43, produced a profile similar to the exogenous application of NAAG. ZJ43 (30–60 nA) produced a robust enhancement of Delay cell firing (30 nA vs. control, $P = 0.0011$; 60 nA vs. control, $P = 0.01$; 60 nA vs. 30 nA, $P = 0.22$; Fig. 8*A*,*B*). Neuronal firing during the delay period was preferentially increased for the neurons' preferred direction, thus increasing d' measures of spatial tuning (30 nA vs. control, $P = 0.003$; 60 nA vs. control, $P = 0.005$; 60 nA vs. 30 nA, $P = 0.89$; Fig. 8*B*). The enhancing effects of ZJ43 (30 nA) on Delay cell firing and spatial tuning were reversed by co-iontophoresis of the cAMP analog, 8-Bromo-cAMP with ZJ43 (ZJ43@30 nA vs. control, $P = 0.017$; 8-Bromo-cAMP@10 nA + ZJ43@30 nA vs. ZJ43@30 nA, $P = 0.026$; Fig. 8*C*,*D*), consistent with mGluR3 stimulation enhancing Delay cell firing through inhibition of cAMP-K^+ channel signaling.

mGluR2 Stimulation has an Inverted-U Effect on Delay Cell Firing

In contrast to the uniformly enhancing effects of NAAG and ZJ43, the mGluR2 PAM, BINA, produced an inverted-U dose–response on

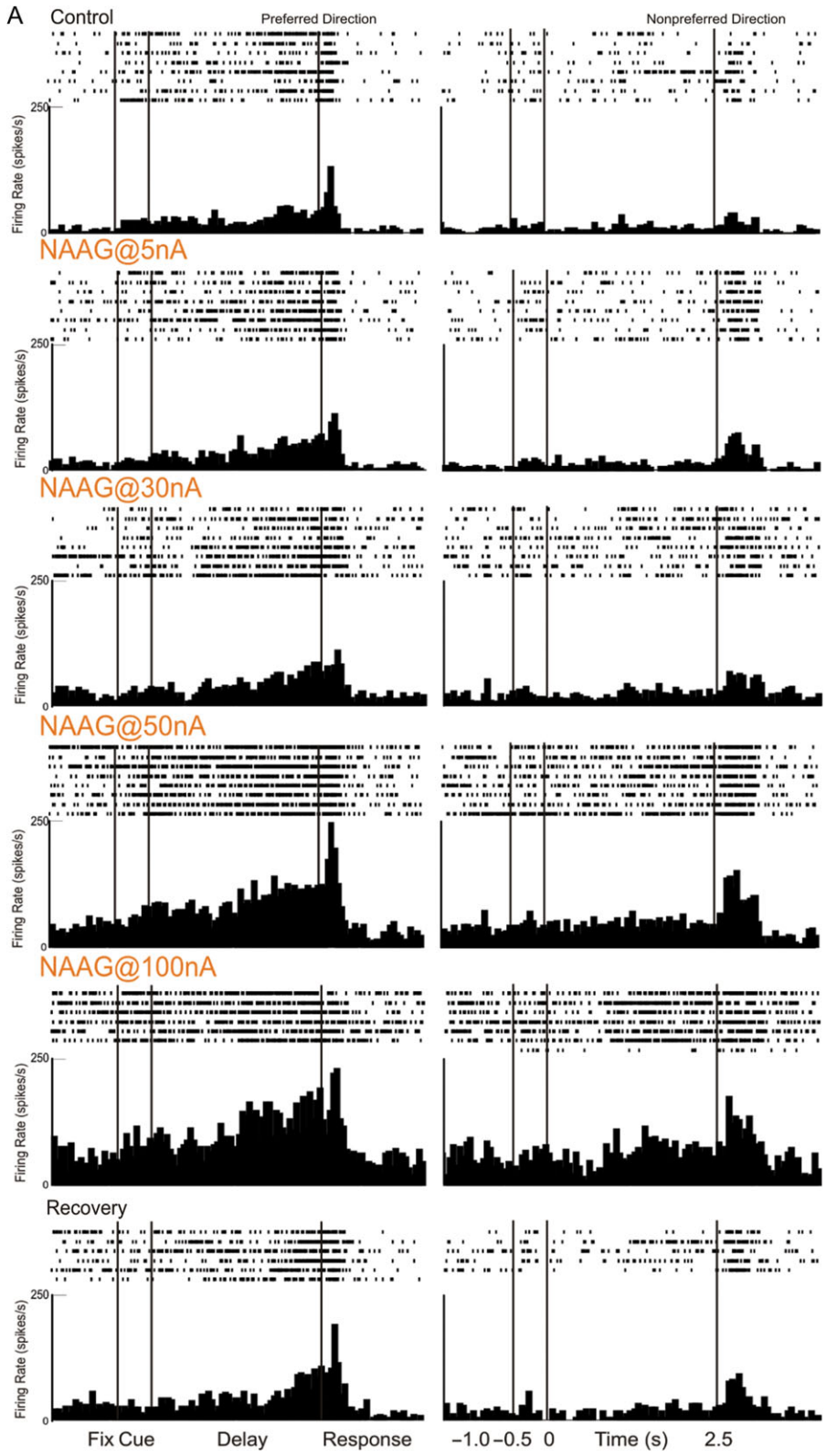

Figure 7. mGluR3 stimulation by iontophoresis of NAAG enhances Delay cell firing. (*A*) Example of a Delay cell where NAAG had a linear, enhancing effect on neuronal firing. The increase was significant even when the dose was raised to 100 nA; firing recovered to control levels after washout. (*B*) The averaged neuronal firing rate during the delay epoch for the population of Delay cells ($n = 22$) under Control, NAAG low-dose condition (5–30 nA) and NAAG high-dose condition (50–100 nA), shown for the neurons' preferred direction (solid line), and a representative nonpreferred direction (dashed line); mean ± SEM. Both low and high doses significantly increased delay firing, especially for the neuron's preferred direction. (*C*) The averaged d' for neuronal firing during the delay epoch for the population of Delay cells under Control, NAAG low-dose, and NAAG high-dose conditions; mean + SEM. Both low and high doses of NAAG enhanced the neural representation of visual space as measured by d'. $^{*}P < 0.05$, $^{**}P < 0.01$, $^{***}P < 0.001$, n.s. nonsignificant, compared with Control condition.

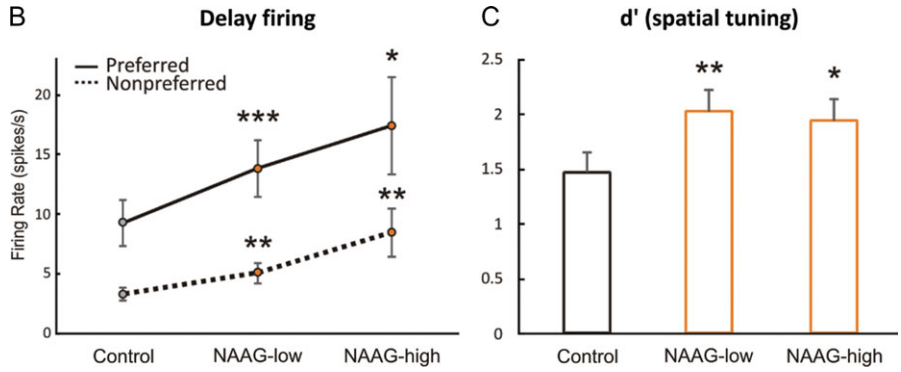

Figure 7. *Continued.*

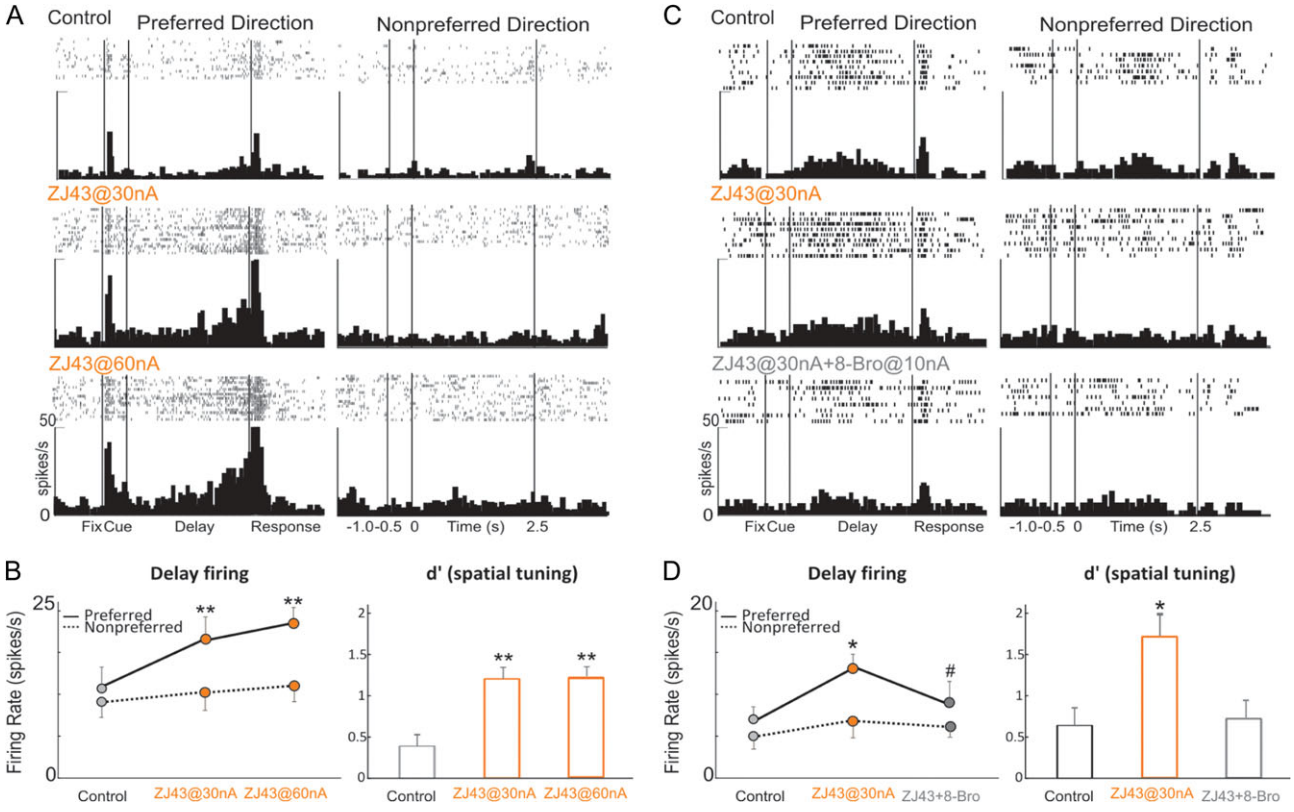

Figure 8. Increasing endogenous NAAG stimulation of mGluR3 by iontophoresis of the glutamate carboxypeptidase II inhibitor, ZJ43, enhances Delay cell firing, and is reversed by 8-Bromo-cAMP. (*A*) Example of a Delay cell where ZJ43 had a linear, enhancing effect on neuronal firing. (*B*) The averaged neuronal firing rate (left) and d' for neuronal firing (right) during the delay epoch for the population of Delay cells ($n = 6$) under Control, ZJ43@30 nA, and ZJ43@60 nA conditions, shown for the neurons' preferred direction (solid line), and a representative nonpreferred direction (dashed line); mean ± SEM. Both doses significantly increased delay firing for the neuron's preferred direction and enhanced the neural representation of visual space as measured by d'. (*C*) Example of a Delay cell where 8-Bromo-cAMP reversed the enhancing effect of ZJ43 on neuronal firing. (*D*) The averaged neuronal firing rate (left) and d' for neuronal firing (right) during the delay epoch for the population of Delay cells ($n = 4$) under Control, ZJ43@30 nA and ZJ43@30 nA + 8-Bromo-cAMP@10 nA conditions, shown for the neurons' preferred direction (solid line), and a representative nonpreferred direction (dashed line); mean ± SEM. Co-iontophoresis of 8-Bromo-cAMP with ZJ43 reversed the enhancing effects of ZJ43 (30 nA) on Delay cell firing and spatial tuning. $^{*}P < 0.05$, $^{**}P < 0.01$ compared with Control condition; $^{\#}P < 0.05$ compared with ZJ43 alone.

Delay cell firing that can be seen in an individual neuron (Fig. 9*A*), and in the averaged population responses (Fig. 9*B*,*C*; 1-ANOVA-R, $F(2,24) = 4.06$, $P = 0.03$; quadratic trend, $F(1,12) = 9.127$, $P = 0.011$). The inverted-U was also evident in d' measures of spatial tuning (1-ANOVA-R, $F(2,24) = 3.752$, $P = 0.038$; quadratic trend, $F(1,12) = 4.789$, $P = 0.049$). Thus, iontophoresis of low doses (5–40 nA) of BINA increased Delay cell firing ($n = 34$), with prominent effects on the neurons' preferred direction (Fig. 9*B*; $t_{dep}(33) = -3.996$, $P < 0.001$), leading to larger measures of spatial tuning (Fig. 9*C*; 2-ANOVA-R, $F_{direction \times drug}(1,33) = 9.906$, $P = 0.003$; d' increased $t_{dep}(33) = -2.530$, $P = 0.016$). In contrast, higher BINA doses (50–100 nA) greatly reduced neuronal firing compared with low doses (Fig. 9*B*; $n = 13$, $t_{dep}(12) = 2.755$, $P = 0.017$) and eroded d' measures of spatial tuning (Fig. 9*C*; $t_{dep}(12) = 3.152$, $P = 0.008$), such that they no longer differed from control ($P > 0.1$). The reduction in firing was most evident when BINA doses were increased to 50–100 nA, but could occasionally be seen with a lower dose, for example, 30 nA (Fig. 9*A*). Thus, low doses of the mGluR2 PAM,

BINA, increased Delay cell firing and enhanced spatial tuning, whereas higher doses eroded these improving effects.

Effects of Systemically Administered BINA on Working Memory Performance

As NAAG cannot be administered systemically, and there are currently no mGluR3-selective PAMs, behavioral studies focused on the mGluR2 PAM, BINA. The effects of systemic administration of BINA on spatial working memory performance in young adult and aged monkeys were consistent with the electrophysiological data, showing an inverted-U dose–response (Fig. 9*D*; n = 12, 1-ANOVA-R on doses 0.0001–0.05 mg/kg: significant quadratic trend for polynomial contrasts $F(1,11) = 6.402$, $P = 0.028$; no overall significant effect of BINA, $F(4,44) = 1.458$, $P = 0.231$). Monkeys (n = 12) received BINA doses between 0.0001 and 0.05 mg/kg; there was a small but significant improvement in delayed response performance following the 0.001 mg/kg dose (Fig. 9*D*, $t_{dep}(11) = -2.218$, $P = 0.049$), but improvement became inconsistent when the dose was raised. A smaller subset of monkeys (n = 5–11) received higher doses (up to 1.0 mg/kg), but these doses had mixed effects (all $P > 0.1$). For 11 of the 12 monkeys tested, a dose of BINA could be found that reliably improved performance above baseline vehicle performance (Fig. 9*D*, "best dose" vs. vehicle, $t_{dep}(11) = -11.849$, $P < 0.001$). No side effects were observed. Modest improvement was observed following BINA in both young adult (Fig. 9*E*), and aged monkeys (Fig. 9*F*), with no apparent age-related differences in drug potency or efficacy ($P > 0.1$). It is noteworthy that the beneficial effects of BINA in monkeys were less robust than improvements seen with systemic administration of mixed mGluR2/3 agonists (Jin et al. 2016), suggesting an important role for mGluR3.

Discussion

This study is the first dissection of mGluR2 versus mGluR3 mechanisms in the higher cognitive circuits of primate dlPFC that generate the mental representations underlying working memory. The data indicate that mGluR3 is especially positioned to strengthen these cognitive circuits, and thus genetic

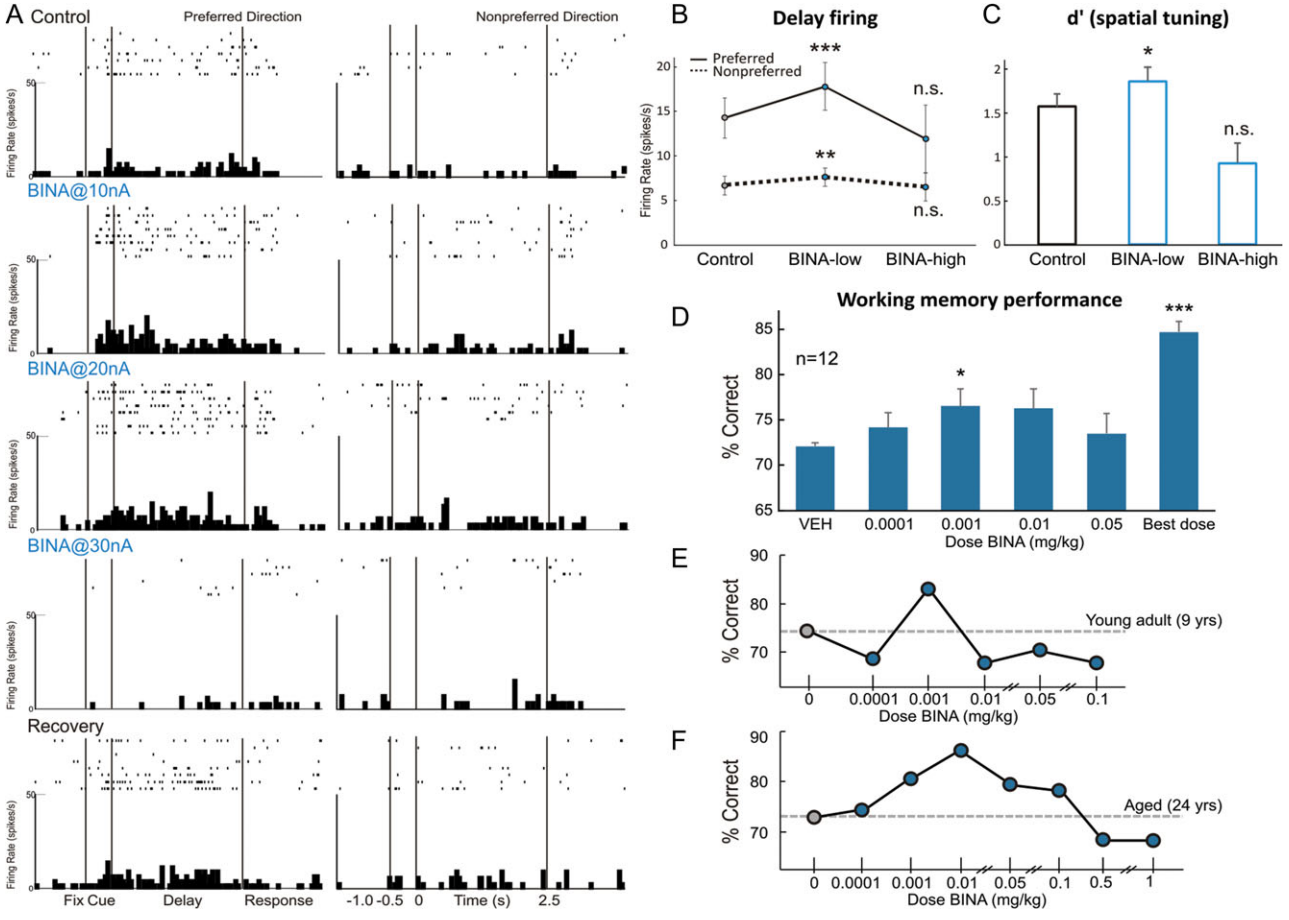

Figure 9. mGluR2 stimulation with BINA has an inverted-U dose–response effect on Delay cell neuronal firing rates, d' measures of Delay cell spatial tuning, and working memory performance in monkeys. (*A*) Example of a Delay cell where iontophoresis of low doses of BINA (10 and 20 nA) increased Delay cell firing, whereas a higher dose of 30 nA greatly reduced the firing. Neuronal firing recovered to control levels after drug washout. (*B*) The averaged neuronal firing rate during the delay epoch for the population of Delay cells under Control, BINA low-dose condition (5–40 nA), and BINA high-dose condition (50–100 nA). Averaged firing rate is shown for the neurons' preferred direction (solid line) and a representative nonpreferred direction (dashed line); mean ± SEM. Low doses increased while higher doses reduced Delay cell firing. (*C*) The averaged d' measure of spatial tuning for neuronal firing during the delay epoch for the population of Delay cells under Control, BINA low-dose condition (5–40 nA), and BINA high-dose condition (50–100 nA); mean + SEM. Low doses improved while higher doses reduced d'. (*D*) Average percent correct on the delayed response task following systemically administered BINA or vehicle control; mean + SEM, n = 12. BINA produced an inverted-U dose–response, with modest improvement at lower doses. (*E*,*F*) Individual examples of dose–response curves of a young adult (*E*) and an aged monkey (*F*), where BINA produced an inverted-U dose–response influence on working memory performance. *$P < 0.05$, **$P < 0.01$, ***$P < 0.001$, n.s. nonsignificant, compared with Control condition.

or environmental insults to these receptors would contribute to higher cognitive dysfunction.

mGluR2 versus mGluR3 Influences on Layer III dlPFC Working Memory Circuits

mGluR3 is prominently localized in layer III dlPFC dendritic spines at the synapse and/or near the spine apparatus, positioned to inhibit feedforward Ca^{2+}-cAMP-K^+ channel signaling, and to strengthen dlPFC network firing (Fig. 1*D*). mGluR2 is predominantly an autoreceptor, positioned presynaptically to reduce glutamate release and decrease neuronal firing (Fig. 1*D*), similar to that seen in layer V of rat medial PFC (Benneyworth et al. 2007). This pattern of mGluR2 versus mGluR3 localization in primate layer III dlPFC is consistent with the physiological and behavioral data, where the agents that increased mGluR3 stimulation uniformly enhanced firing, while the mGluR2 PAM, BINA, produced an inverted-U dose–response. Interestingly, BINA produced much weaker enhancement than mixed mGluR2/3 agonists, where low doses of APDC or LY379268 markedly improved working memory performance and produced large increases in Delay cell firing (Jin et al. 2016). These findings suggest that the beneficial effects of mixed mGluR2/3 compounds involved actions at mGluR3. The enhancing effects of APDC (Jin et al. 2016) and ZJ43 (this study) were reversed by the cAMP analog, 8-Bromo-cAMP, consonant with mGluR3 strengthening dlPFC network connections by inhibiting cAMP-K^+ channel signaling in postsynaptic spines.

mGluR2/3 have been shown at postsynaptic sites in rodents (Petralia et al. 1996; Tamaru et al. 2001), but have been a minor focus of most research, where studies have focused on presynaptic actions (e.g., Benneyworth et al. 2007). Layer III PFC circuits expand greatly over evolution, with large increases in the number of glutamate connections on dendritic spines (Elston 2003). The current data indicate that the role of mGluR3 expanded in parallel with these elaborations, whereby the co-release of NAAG by glutamate axon terminals can amplify NMDAR actions to maintain network firing in the absence of sensory stimulation. The current findings of marked enhancements of Delay cell firing following increases in either endogenous levels of NAAG, or exogenous application of NAAG, are consistent with this view. It is likely that both NAAG and glutamate engage postsynaptic mGluR3 in and near the synapse, increasing dlPFC network firing through inhibition of cAMP-K^+ channel signaling in spines.

Roles in Astrocytes

Group II mGluR also play important roles in astroglial function, including the regulation of glutamate signaling via EAAT expression, structural plasticity, and neuroprotective actions. Research has focused primarily on mGluR3, as early studies stated that astrocytes in rodent brain do not express mGluR2 (Ohishi et al. 1998). A variety of studies show that astroglial mGluR3 protect both neurons and glia (Durand et al. 2011). However, while astroglial mGluR3 is protective against excitotoxicity, neuronal mGluR2 was unexpectedly detrimental (Corti et al. 2007b).

Our data show that mGluR3 is the most prevalent in dlPFC astrocytes, and are targeted at their traditional location in PAPs, positioned to regulate uptake of synaptic glutamate, whereas a limited mGluR2 component is distributed diffusely on astrocytic membranes away from the synapse. These findings raise questions regarding the role of mGluR2 in astrocytes, for example, what functions they perform, and whether they are unique to the primate PFC. Species differences in mGluR2 versus mGluR3 localization will be an important arena for future research.

Clinical Relevance

Layer III dlPFC pyramidal cells are a focus of pathology in many higher cognitive disorders. Postmortem studies of the dlPFC from patients with schizophrenia have shown that layer III pyramidal cells lose dendrites and spines (Glantz and Lewis 2000), and become profoundly hypometabolic (Arion et al. 2015). In imaging studies, dlPFC hypofrontality during a working memory task strongly correlates with symptoms of thought disorder (Perlstein et al. 2001), indicating a link to cardinal cognitive symptoms. Working memory deficits also arise with advancing age, and layer III dlPFC neurons lose thin spines with normal aging (Morrison and Baxter 2012), and undergo neurofibrillary degeneration in AD (Morrison and Baxter 2012).

Accumulating evidence suggests that mGluR3 may have beneficial, protective effects, whereas mGluR2 may be harmful to dlPFC cognitive disorders. Genetic variations in mGluR3 and reduced mGluR3 signaling are increasingly associated with schizophrenia (Egan et al. 2004; Chang et al. 2015), including GWAS validation (Schizophrenia Working Group of the Psychiatric Genomics Consortium 2014). Early studies found increased expression of mGluR3 variants (Sartorius et al. 2008), and decreased expression of mGluR3 dimers (Corti et al. 2007a) in dlPFC. Importantly, a comprehensive postmortem study of brains from patients with schizophrenia found reduced mGluR3 expression, but unchanged mGluR2, in dlPFC but not in other cortical regions (Ghose et al. 2009). This same study reported increased dlPFC expression of glutamate carboxypeptidase II, the extracellular enzyme that catabolizes NAAG, suggesting that these individuals may have had less endogenous NAAG to stimulate mGluR3 in dlPFC (Ghose et al. 2009). The authors speculated that inadequate postsynaptic mGluR3 signaling may contribute to schizophrenia, and this study provides the first, direct support for this hypothesis, demonstrating that increasing NAAG stimulation of mGluR3 by direct application or by inhibition of glutamate carboxypeptidase II enhances Delay cell firing. As glutamate carboxypeptidase II inhibitors have been shown to improve memory and protect neural circuits from injury in rodent models (Rahn et al. 2012; Janczura et al. 2013; Gao et al. 2015), they may have widespread therapeutic potential.

Of immediate relevance to our data showing beneficial influences of mGluR3 in dlPFC spines, GRM3 variants that weaken receptor function have been linked to (1) poorer PFC cognitive function in patients with schizophrenia (Egan et al. 2004; Mössner et al. 2008; Jablensky et al. 2011; Chang et al. 2015; Kinoshita et al. 2015), (2) altered activation of dlPFC during performance of cognitive tasks (Egan et al. 2004; Kinoshita et al. 2015), (3) disorganized PFC white matter (Mounce et al. 2014), and (4) working memory impairments with anti-psychotic medications (Bishop et al. 2015). Alterations in GRM3 have also been linked to increased risk of other disorders, for example, bipolar disorder (O'Brien et al. 2014) and autism spectrum illness (Hadley et al. 2014). Thus, there is a large body of literature linking mGluR3 to mental disorders associated with impaired PFC function.

mGluR3 is also increasingly linked to age-related cognitive disorders. There is a decline in mGluR3 expression with advancing age in human PFC (Colantuoni et al. 2008). As mGluR3 is protective against the formation of Aβ in vitro (Caraci et al. 2011), age-related loss of mGluR3 may contribute to increasing Aβ. Neuronal mGluR3 in dlPFC may also ameliorate AD pathology by

inhibiting cAMP-PKA phosphorylation of tau (Carlyle et al. 2014), which aggregates in thin spines near the synapse and spine apparatus, similar to mGluR3 (Fig. 3G). Future research could test whether a selective mGluR3 PAM could enhance cell firing and reduce tau phosphorylation in aging dlPFC.

In contrast to mGluR3, a variety of data suggest that mGluR2 may be detrimental to higher cognitive abilities. Methylation of the promoter region of GRM2, which reduces mGluR2 expression, lowers the risk of schizophrenia, suggesting that its actions are harmful to cognitive health (Kordi-Tamandani et al. 2013). Furthermore, mGluR2 stimulation increases Aβ release from presynaptic terminals (Kim et al. 2010; Caraci et al. 2011). Thus, despite the structural and signaling similarities in these receptors, mGluR2 and mGluR3 appear to serve disparate functions.

Our understanding of glutamate mechanisms has begun to shift as we learn more about glutamate actions in primate cerebral cortex. Based on cell culture and rodent models, mGluR2/3 agonists and mGluR2 PAMs were originally developed as potential therapeutics to reduce excitotoxicity. However, we have recently learned that layer III Delay cells in monkey dlPFC show reduced firing under conditions of stress, NMDAR blockade or with advancing age (Arnsten et al. 2012; Morrison and Baxter 2012; Wang et al. 2013), and are metabolically underactive in schizophrenia (Arion et al. 2015) and AD (Young-Collier et al. 2012). Thus, instead of focusing on presynaptic mGluR2 targets to reduce glutamate release, a superior therapeutic strategy may be to strengthen the connections of higher cognitive networks through stimulation of postsynaptic mGluR3. This study suggests that this may be best accomplished through the development of agents that selectively activate mGluR3. A recent meta-analysis of mGluR2/3 agonist actions in patients with schizophrenia demonstrates that low doses are efficacious in patients in early, but not late, stages of the illness (Kinon et al. 2015). Our data suggest that the low doses may have acted preferentially at postsynaptic mGluR3 (and possibly mGluR2) on dlPFC spines, and that loss of these spines with disease progression may remove the substrate for therapeutic drug actions. Better understanding of the individual contribution of mGluR2 versus mGluR3 in primate dlPFC will help to refine more effective therapeutic strategies.

Supplementary Material

Supplementary material are available at *Cerebral Cortex* online.

Funding

Public Health Service grants R01AG043430-02 and R01MH100064-01A1 to A.F.T.A., and donations to L.E.J. in memory of Percy Sanguinetti Arnsten and to C.D.P. in memory of Elsie Louise Torrance Higgs, whose courage inspired this work.

Notes

We thank L. Ciavarella, S. Johnson, T. Sadlon, M. Wilson, and M. Horn for their invaluable technical support. *Conflict of Interest*: None declared.

References

Arion D, Corradi JP, Tang S, Datta D, Boothe F, He A, Cacace AM, Zaczek R, Albright CF, Tseng GF, et al. 2015. Distinctive transcriptome alterations of prefrontal pyramidal neurons in schizophrenia and schizoaffective disorder. Mol Psychiatry. 20:1397–1405.

Arnsten AFT, Wang M, Paspalas CD. 2012. Neuromodulation of thought: flexibilities and vulnerabilities in prefrontal cortical network synapses. Neuron. 76:223–239.

Aronica E, Gorter JA, Ijlst-Keizers H, Rozemuller AJ, Yankaya B, Leenstra S, Troost D. 2003. Expression and functional role of mGluR3 and mGluR5 in human astrocytes and glioma cells: opposite regulation of glutamate transporter proteins. Eur J Neurosci. 17:2106–2118.

Benneyworth MA, Xiang Z, Smith RL, Garcia EE, Conn PJ, Sanders-Bush E. 2007. A selective positive allosteric modulator of metabotropic glutamate receptor subtype 2 blocks a hallucinogenic drug model of psychosis. Mol Pharmacol. 72:477–484.

Bishop JR, Reilly JL, Harris MS, Patel SR, Kittles R, Badner JA, Prasad KM, Nimgaonkar VL, Keshavan MS, Sweeney JA. 2015. Pharmacogenetic associations of the type-3 metabotropic glutamate receptor (GRM3) gene with working memory and clinical symptom response to antipsychotics in first-episode schizophrenia. Psychopharmacology. 232:145–154.

Caraci F, Molinaro G, Battaglia G, Giuffrida ML, Riozzi B, Traficante A, Bruno V, Cannella M, Merlo S, Wang X, et al. 2011. Targeting group II metabotropic glutamate (mGlu) receptors for the treatment of psychosis associated with Alzheimer's disease: selective activation of mGlu2 receptors amplifies beta-amyloid toxicity in cultured neurons, whereas dual activation of mGlu2 and mGlu3 receptors is neuroprotective. Mol Pharmacol. 79:618–626.

Carlyle BC, Nairn AC, Wang M, Yang Y, Jin LE, Simen AA, Ramos BP, Bordner KA, Craft GE, Davies P, et al. 2014. cAMP-PKA phosphorylation of tau confers risk for degeneration in aging association cortex. Proc Natl Acad Sci U S A. 111:5036–5041.

Chang M, Sun L, Liu X, Sun W, Ji M, Wang Z, Wang Y, You X. 2015. Evaluation of relationship between GRM3 polymorphisms and cognitive function in schizophrenia of Han Chinese. Psychiatry Res. 229:1043–1046.

Colantuoni C, Hyde TM, Mitkus S, Joseph A, Sartorius L, Aguirre C, Creswell J, Johnson E, Deep-Soboslay A, Herman MM, et al. 2008. Age-related changes in the expression of schizophrenia susceptibility genes in the human prefrontal cortex. Brain Struct Funct. 213:255–271.

Corti C, Crepaldi L, Mion S, Roth AL, Xuereb JH, Ferraguti F. 2007a. Altered dimerization of metabotropic glutamate receptor 3 in schizophrenia. Biol Psychiatry. 62:747–755.

Corti C, Battaglia G, Molinaro G, Riozzi B, Pittaluga A, Corsi M, Mugnaini M, Nicoletti F, Bruno V. 2007b. The use of knockout mice unravels distinct roles for mGlu2 and mGlu3 metabotropic glutamate receptors in mechanisms of neurodegeneration/neuroprotection. J Neurosci. 27:8297–8308.

Durand D, Carniglia L, Caruso C, Lasaga M. 2011. Reduced cAMP, Akt activation and p65-c-Rel dimerization: mechanisms involved in the protective effects of mGluR3 agonists in cultured astrocytes. PLoS One. 6:e22235.

Egan MF, Straub RE, Goldberg TE, Yakub I, Callicott JH, Hariri AR, Mattay VS, Bertolino A, Hyde TM, Shannon-Weickert C, et al. 2004. Variation in GRM3 affects cognition, prefrontal glutamate, and risk for schizophrenia. Proc Natl Acad Sci U S A. 101:12604–12609.

Elston GN. 2003. Cortex, cognition and the cell: new insights into the pyramidal neuron and prefrontal function. Cereb Cortex. 13:1124–1138.

Gao Y, Xu S, Cui Z, Zhang M, Lin Y, Cai L, Wang Z, Luo X, Zheng Y, Wang Y, et al. 2015. Mice lacking glutamate carboxypeptidase II develop normally, but are less susceptible to traumatic brain injury. J Neurochem. 134:340–353.

Ghose S, Gleason KA, Potts BW, Lewis-Amezcua K, Tamminga CA. 2009. Differential expression of metabotropic glutamate receptors 2 and 3 in schizophrenia: a mechanism for antipsychotic drug action? Am J Psychiatry. 166:812–820.

Glantz LA, Lewis DA. 2000. Decreased dendritic spine density on prefrontal cortical pyramidal neurons in schizophrenia. Arch Gen Psychiatry. 57:65–73.

Goldman-Rakic PS. 1995. Cellular basis of working memory. Neuron. 14:477–485.

Hadley D, Wu ZL, Kao C, Kini A, Mohamed-Hadley A, Thomas K, Vazquez L, Qiu H, Mentch F, Pellegrino R, et al. 2014. The impact of the metabotropic glutamate receptor and other gene family interaction networks on autism. Nat Commun. 5:4074.

Harrison PJ, Lyon L, Sartorius LJ, Burnet PW, Lane TA. 2008. The group II metabotropic glutamate receptor 3 (mGluR3, mGlu3, GRM3): expression, function and involvement in schizophrenia. J Psychopharmacol. 22:308–322.

Jablensky A, Morar B, Wiltshire S, Carter K, Dragovic M, Badcock JC, Chandler D, Peters K, Kalaydjieva L. 2011. Polymorphisms associated with normal memory variation also affect memory impairment in schizophrenia. Genes Brain Behav. 10:410–417.

Janczura KJ, Olszewski RT, Bzdega T, Bacich DJ, Heston WD, Neale JH. 2013. NAAG peptidase inhibitors and deletion of NAAG peptidase gene enhance memory in novel object recognition test. Eur J Pharmacol. 701:27–32.

Jin LE, Wang M, Yang S-Y, Yang Y, Galvin VC, Lightbourne TC, Ottenheimer D, Zhong Q, Stein J, Raja A, et al. 2016. mGluR2/3 mechanisms in primate dorsolateral prefrontal cortex: evidence for both presynaptic and postsynaptic actions. Mol Psychiatry. doi:10.1038/mp.2016.129.

Kim SH, Fraser PE, Westaway D, St George-Hyslop PH, Ehrlich ME, Gandy S. 2010. Group II metabotropic glutamate receptor stimulation triggers production and release of Alzheimer's amyloid(beta)42 from isolated intact nerve terminals. J Neurosci. 30:3870–3875.

Kinon BJ, Millen BA, Zhang L, McKinzie DL. 2015. Exploratory analysis for a targeted patient population responsive to the metabotropic glutamate 2/3 receptor agonist pomaglumetad methionil in schizophrenia. Biol Psychiatry. 78:754–762.

Kinoshita A, Takizawa R, Koike S, Satomura Y, Kawasaki S, Kawakubo Y, Marumo K, Tochigi M, Sasaki T, Nishimura Y, et al. 2015. Effect of metabotropic glutamate receptor-3 variants on prefrontal brain activity in schizophrenia: An imaging genetics study using multi-channel near-infrared spectroscopy. Prog Neuropsychopharmacol Biol Psychiatry. 62:14–21.

Kordi-Tamandani DM, Dahmardeh N, Torkamanzehi A. 2013. Evaluation of hypermethylation and expression pattern of GMR2, GMR5, GMR8, and GRIA3 in patients with schizophrenia. Gene. 515:163–166.

Morrison JH, Baxter MG. 2012. The ageing cortical synapse: hallmarks and implications for cognitive decline. Nat Rev Neurosci. 13:240–250.

Mössner R, Schuhmacher A, Schulze-Rauschenbach S, Kühn KU, Rujescu D, Rietschel M, Zobel A, Franke P, Wölwer W, Gaebel W, et al. 2008. Further evidence for a functional role of the glutamate receptor gene GRM3 in schizophrenia. Eur Neuropsychopharmacol. 18:768–772.

Mounce J, Luo L, Caprihan A, Liu J, Perrone-Bizzozero NI, Calhoun VD. 2014. Association of GRM3 polymorphism with white matter integrity in schizophrenia. Schizophr Res. 155:8–14.

Neale JH, Olszewski RT, Zuo D, Janczura KJ, Profaci CP, Lavin KM, Madore JC, Bzdega T. 2011. Advances in understanding the peptide neurotransmitter NAAG and appearance of a new member of the NAAG neuropeptide family. J Neurochem. 118:490–498.

O'Brien NL, Way MJ, Kandaswamy R, Fiorentino A, Sharp SI, Quadri G, Alex J, Anjorin A, Ball D, Cherian R, et al. 2014. The functional GRM3 Kozak sequence variant rs148754219 affects the risk of schizophrenia and alcohol dependence as well as bipolar disorder. Psychiatr Genet. 24:277–278.

Ohishi H, Neki A, Mizuno N. 1998. Distribution of a metabotropic glutamate receptor, mGluR2, in the central nervous system of the rat and mouse: an immunohistochemical study with a monoclonal antibody. Neurosci Res. 30:65–82.

Paspalas CD, Wang M, Arnsten AF. 2013. Constellation of HCN Channels and cAMP regulating proteins in dendritic spines of the primate prefrontal cortex: potential substrate for working memory deficits in schizophrenia. Cereb Cortex. 23: 1643–1654.

Perlstein WM, Carter CS, Noll DC, Cohen JD. 2001. Relation of prefrontal cortex dysfunction to working memory and symptoms in schizophrenia. Am J Psychiatry. 158:1105–1113.

Petralia RS, Wang YX, Niedzielski AS, Wenthold RJ. 1996. The metabotropic glutamate receptors, mGluR2 and mGluR3, show unique postsynaptic, presynaptic and glial localizations. Neuroscience. 71:949–976.

Rahn KA, Watkins CC, Alt J, Rais R, Stathis M, Grishkan I, Crainiceau CM, Pomper MG, Rojas C, Pletnikov MV, et al. 2012. Inhibition of glutamate carboxypeptidase II (GCPII) activity as a treatment for cognitive impairment in multiple sclerosis. Proc Natl Acad Sci U S A. 109:20101–20106.

Sartorius LJ, Weinberger DR, Hyde TM, Harrison PJ, Kleinman JE, Lipska BK. 2008. Expression of a GRM3 splice variant is increased in the dorsolateral prefrontal cortex of individuals carrying a schizophrenia risk SNP. Neuropsychopharmacology. 33:2626–2634.

Schizophrenia Working Group of the Psychiatric Genomics Consortium. 2014. Biological insights from 108 schizophrenia-associated genetic loci. Nature. 511:421–427.

Tamaru Y, Nomura S, Mizuno N, Shigemoto R. 2001. Distribution of metabotropic glutamate receptor mGluR3 in the mouse CNS: differential location relative to pre- and postsynaptic sites. Neuroscience. 106:481–503.

Tanabe Y, Masu M, Ishii T, Shigemoto R, Nakanishi S. 1992. A family of metabotropic glutamate receptors. Neuron. 8: 169–179.

Wang M, Gamo NJ, Yang Y, Jin LE, Wang XJ, Laubach M, Mazer JA, Lee D, Arnsten AFT. 2011. Neuronal basis of age-related working memory decline. Nature. 476:210–213.

Wang M, Yang Y, Wang CJ, Gamo NJ, Jin LE, Mazer JA, Morrison JH, Wang X-J, Arnsten AF. 2013. NMDA receptors subserve working memory persistent neuronal firing In dorsolateral prefrontal cortex. Neuron. 77:736–749.

Wang M, Ramos BP, Paspalas CD, Shu Y, Simen A, Duque A, Vijayraghavan S, Brennan A, Dudley A, Nou E, et al. 2007. Alpha2A-adrenoceptors strengthen working memory networks by inhibiting cAMP-HCN channel signaling in prefrontal cortex. Cell. 129:397–410.

Young-Collier KJ, McArdle M, Bennett JP. 2012. The dying of the light: mitochondrial failure in Alzheimer's disease. J Alzheimers Dis. 28:771–781.